Notes on force of gas on particles in CE simulations

Luke Chamandy

May 24, 2019

1 Calculation of drag force

1.1 Preliminary comments

From Wikipedia: *In fluid dynamics, drag (sometimes called air resistance, a type of friction, or fluid resistance, another type of friction or fluid friction) is a force acting opposite to the relative motion of any object moving with respect to a surrounding fluid.*

So technically, the drag involves the relative velocity between fluid and particle. Thus far, we have not attempted to calculate the relative velocity between particle and gas or its direction. This would involve taking some average over the gas near the particle. But which region should be chosen? Should it be a weighted average? A related issue is that in the Bondi-Hoyle-Lyttleton (BHL) problem, the velocity that goes into the formula for gas dynamical friction is the relative velocity of the particle and the unperturbed ambient medium at infinity. Thus it is non-trivial to calculate or even define, in the simulation, the relative velocity.

To measure from the simulation the component of the gas dynamical friction force along the relative velocity between particle and gas, we do not need the magnitude of the velocity, just the direction.

In any case, we consider two velocities below. Either (i) we measure the component of the force in the direction of the velocity of the particle in the simulation (lab) frame (equal to the relative velocity if the average gas velocity is 0 in the lab frame), or (ii) we measure the component of the force in the direction of the velocity of one particle with respect to the other particle. This would be equal to the relative velocity of particle and gas if the gas was moving along with the other particle. The velocity (ii) is in general greater than (i). In the idealization that the envelope is not rotating and continues to orbit with particle 1 at its center, velocity (ii) would be the relative velocity between particle 2 and gas. The envelope actually would lag the core, so (ii) is probably an overestimate, but on the other hand gas gets accelerated (and slighshotted) as it approaches particle 2. In the early stages, the relative velocity between particle 1 and gas is basically 0, while the velocity between particle 2 and gas is close to velocity (ii) since the envelope is not rotating initially. In the late stages, the relative velocity between each particle and the gas is probably smaller than (i) because of gas round the particle orbiting along with the particle. We can also measure the component of the force tangential to the line joining the particles (the ϕ-component). However, for analytical estimates from BHL theory, we need the magnitude.

To make contact with other approaches for CEE, e.g. MacLeod et al. (2017) to measure the drag force on particle 2, it is reasonable to either use the velocity of particle 2 with respect to particle 1 or the ϕ-component of that velocity. These are the same for circular orbits, and the orbit is approximated to be circular in many studies.

Another possibility is to calculate the orbital velocity of particle 2 with respect to particle 1 at a given separation, assuming that the envelope remains unperturbed, assuming a circular orbit, and taking into account only the envelope mass inside the orbit at a given time and the core mass.

One approach is just to measure the magnitude of the total dynamical friction force from the simulation, which is an upper limit on any individual component of itself.

Then, to take the most favourable value of the relative velocity that would give the smallest value of the drag according to BHL theory. If the BHL force is *still* much larger than the force we measure in the simulation, then we can be sure that simulation and theory do not agree.

1.2 Drag force in simulation (lab) inertial frame

Drag force on particle i:

$$F_{\mathrm{d},i} = \frac{\boldsymbol{f}_i \cdot \boldsymbol{v}_i}{v_i} = \frac{f_{i,x}v_{i,x} + f_{i,y}v_{i,y} + f_{i,z}v_{i,z}}{v_i}, \tag{1}$$

where $\boldsymbol{f}_i$ is the net force exerted on particle i by the gravitational interaction with all gas in the simulation domain,

$$\boldsymbol{f}_i = \mathrm{G}m_i \sum_V \rho(\boldsymbol{s}) \frac{\boldsymbol{s} - \boldsymbol{s}_i}{|\boldsymbol{s} - \boldsymbol{s}_i|^3} d^3s, \tag{2}$$

where m_i is the mass of particle i, ρ is the gas density, V is the volume of the simulation domain, and $\boldsymbol{s} = x\hat{\boldsymbol{x}} + y\hat{\boldsymbol{y}} + z\hat{\boldsymbol{z}}$ and $\boldsymbol{s}_i = x\hat{\boldsymbol{x}}_i + y\hat{\boldsymbol{y}}_i + z\hat{\boldsymbol{z}}_i$ are the positions of the gas element, and particle, respectively. Also,

$$v_i = |\boldsymbol{v}_i| = (v_{i,x}^2 + v_{i,y}^2 + v_{i,z}^2)^{1/2}. \tag{3}$$

Note that as we have defined it, $F_{\mathrm{d},i} < 0$ means a drag force with magnitude $|F_{\mathrm{d},i}|$, while $F_{\mathrm{d},i} > 0$ means a thrust force.

1.3 Drag force in non-inertial frame of one of the particles

The drag force on particle 2 in the reference frame of particle 1 is given by

$$F_{2,\mathrm{drag},1} = \frac{\boldsymbol{f}_2 \cdot (\boldsymbol{v}_2 - \boldsymbol{v}_1)}{v_{2,1}} = \frac{f_{2,x}(v_{2,x} - v_{1,x}) + f_{2,y}(v_{2,y} - v_{1,y}) + f_{2,z}(v_{2,z} - v_{1,z})}{v_{2,1}}, \tag{4}$$

where

$$v_{2,1} = ((v_{2,x} - v_{1,x})^2 + (v_{2,y} - v_{1,y})^2 + (v_{2,z} - v_{1,z})^2)^{1/2}. \tag{5}$$

The drag force on particle 1 in the reference frame of particle 2 is obtained by interchanging indices 1 and 2.

1.4 ϕ-component of force on particle due to gravitational interaction with gas

For some applications, we would like to calculate the component of the force on particle i due to the gas that is tangential to the line joining the particles and paralle to the orbital plane (which we will assume to be parallel to the $z = 0$ plane–this assumption is normally fine but should be checked for each simulation). Thus, we need to convert from Cartesian (x, y, z) to cylindrical (r, ϕ, z) coordinates and then select the ϕ-component. Define $r = [(x_i - x_j)^2 + (y_i - y_j)^2]^{1/2}$, the unit vector $\hat{\boldsymbol{r}} = [(x_i - x_j)\hat{\boldsymbol{x}} + (y_i - y_j)\hat{\boldsymbol{y}}]/r$ and the projection, in the orbital plane, of the vector from particle j to particle i is $\boldsymbol{r} = r\hat{\boldsymbol{r}}$.

The force in equation (2) can be written as

$$\boldsymbol{f}_i = A\hat{\boldsymbol{r}} + B\hat{\boldsymbol{\phi}} + C\hat{\boldsymbol{z}} \tag{6}$$

We want to know the ϕ-component, that is we want to know the value of B. Then we compute

$$\boldsymbol{r} \times \boldsymbol{f}_i = rB\hat{\boldsymbol{z}} - rC\hat{\boldsymbol{\phi}} \tag{7}$$

and take the z-component. That is,

$$f_{i,\phi} = \frac{\boldsymbol{r} \times \boldsymbol{f}_i}{r} \cdot \hat{\boldsymbol{z}}. \tag{8}$$

Now, since the simulation uses Cartesian coordinates, we want the right side written in Cartesian coordinates. Then

$$f_{i,\phi} = \frac{\boldsymbol{r} \times \boldsymbol{f}_i}{r} \cdot \hat{\boldsymbol{z}} = \frac{r_x f_{i,y} - r_y f_{i,x}}{r} = \frac{r_x f_{i,y} - r_y f_{i,x}}{(r_x^2 + r_y^2)^{1/2}} = \frac{(x_i - x_j)f_{i,y} - (y_i - y_j)f_{i,x}}{[(x_i - x_j)^2 + (y_i - y_j)^2]^{1/2}} \tag{9}$$

Likewise, for the radial component parallel to the xy plane we can write,

$$f_{i,r} = \frac{\boldsymbol{r} \cdot \boldsymbol{f}_i}{r} = \frac{r_x f_{i,x} + r_y f_{i,y}}{r} = \frac{r_x f_{i,x} + r_y f_{i,y}}{(r_x^2 + r_y^2)^{1/2}} = \frac{(x_i - x_j)f_{i,x} + (y_i - y_j)f_{i,y}}{[(x_i - x_j)^2 + (y_i - y_j)^2]^{1/2}}. \tag{10}$$

If we are interested in the force along the axis joining particles 1 and 2 (which need not be in the xy plane in general), this is given by

$$f_{i,R} = \frac{\boldsymbol{r} \cdot \boldsymbol{f}_i}{R} = \frac{(x_i - x_j)f_{i,x} + (y_i - y_j)f_{i,y} + (z_i - z_j)f_{i,z}}{[(x_i - x_j)^2 + (y_i - y_j)^2 + (z_i - z_j)^2]^{1/2}}. \tag{11}$$

The ϕ-, r- and R-components of the velocity can be calculated in precisely the same way as the forces.

2 Results

2.1 Comparison of forces obtained using different simulation analysis tools

Table 1: Comparison between values of force components for frame 173 (last frame of simulation, at $t = 40\,\mathrm{d}$), for three different analysis methods: Post-processing using AstroBear (Astrobear PP), VisIt analysis on full simulation data (VisIt full), and the same VisIt analysis on deresolved simulation data (VisIt deresolved).

Component	AstroBear PP	VisIt full	VisIt deresolved
$f_{1,x}$	1.3207×10^{34}	1.3209×10^{34}	1.316×10^{34}
$f_{1,y}$	-8.5798×10^{33}	-8.5806×10^{34}	-8.652×10^{34}
$f_{1,z}$	-3.4892×10^{32}	-3.4959×10^{32}	-3.214×10^{32}
$f_{2,x}$	-1.2274×10^{34}	-1.2274×10^{34}	-1.251×10^{34}
$f_{2,y}$	4.5818×10^{33}	4.5834×10^{33}	4.576×10^{33}
$f_{2,z}$	2.1299×10^{32}	2.1019×10^{32}	-2.918×10^{31}

See Tab. 2.1. The values of the force components for frame 173 (last frame of simulation at $t = 40\,\mathrm{d}$) agree very well between post-processing and VisIt tools for the full resolution data ($< 0.04\%$ difference for x- and y-components). It was

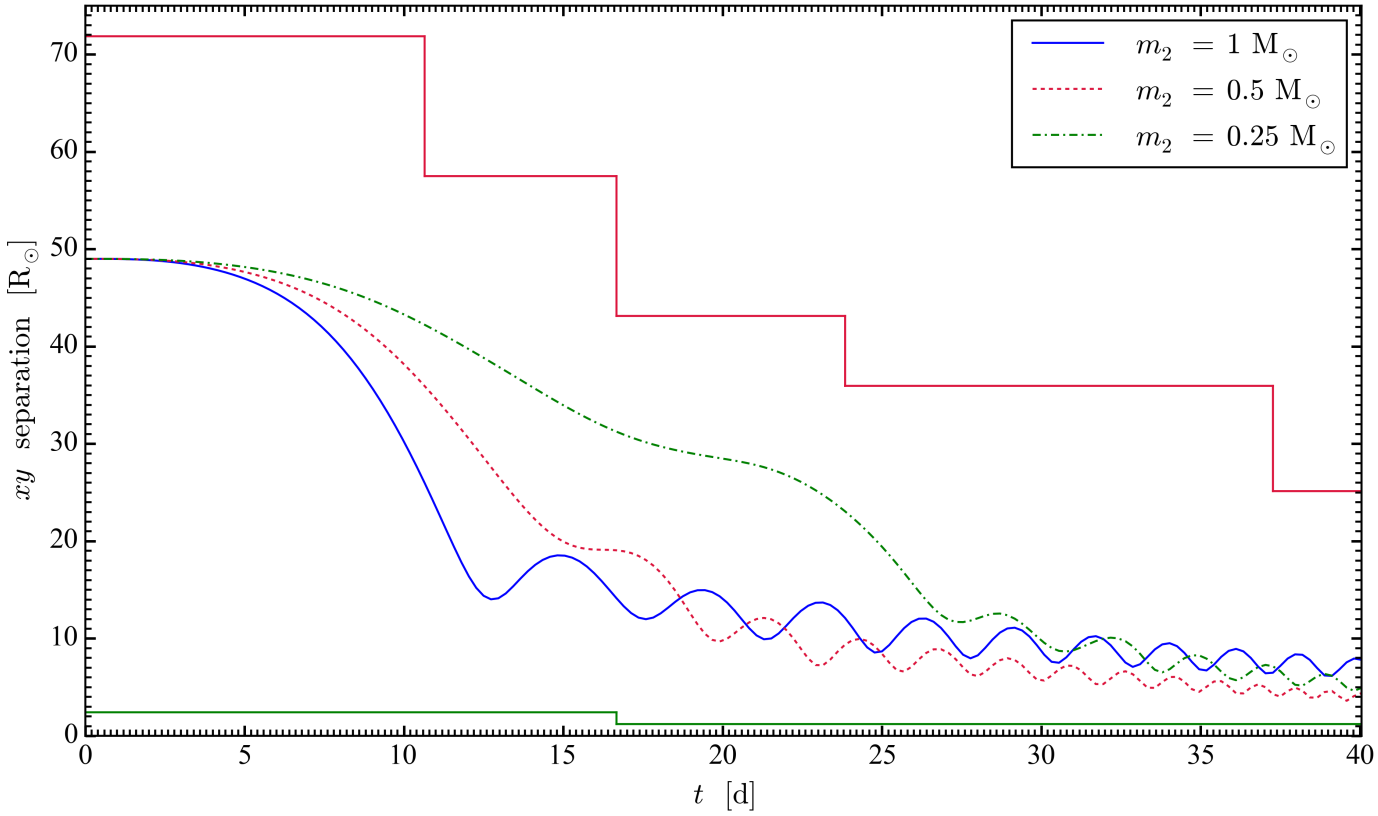

Figure 1: $a(t)$ for Runs 143, 149 and 151.

not possible (due to memory limitations on both Bluehive and Stampede 2) to complete the VisIt analysis using the full data set, but we could do it by first de-resolving the dataset (including only up to maxlevel=3 instead of maxlevel=4 or 5). The agreement for frame 173 is also reasonble between post-processing and VisIt using deresolved data (at the level of 1-2% difference). The figures on the blog post of January 29, 2019 were done using the de-resolved data, analyzed using VisIt. I've redone those figures using postprocessed data and compared the two sets of figures by eye (AstroBear post-processing and VisIt de-resolved) and differences are fairly negligible.

2.2 Forces

2.3 Force as a function of time

Fig. 2: Negative of force of gas on secondary in frame of primary $\boldsymbol{f}_2 \cdot \boldsymbol{v}/v$ is shown by black line. Azimuthal component $f_{2,\phi}$, is shown by orange line. Positive denotes a drag force or force opposite to the azimuthal direction of the orbit, respectively. Note that at early times, $\boldsymbol{f}_2 \cdot \boldsymbol{v}$ is dominated by $f_{2,r} v_r$ since $f_{2,r}$ is so large. At later times the orange and black lines coincide, so $\boldsymbol{f}_2 \cdot \boldsymbol{v}$ is dominated by $f_{2,\phi} v_\phi$. We see that the ϕ-component of the force (orange) is positive during plunge-in (so of opposite sign to the predicted drag force). The secondary is being accelerated around in its orbit by the posterior side of the envelope, which lags the primary particle in its orbit (paper 2). Subsequently, the force is mostly a drag force but oscillates between drag and thrust.

Fig. 3: The same graph is shown for force exerted by gas on particle 1. The force is very small to begin with as the particle sits at the RGB center, but becomes large after plunge-in, when the envelope has been strongly perturbed. At the end of plunge-in and immediately after plunge-in (terminatino of plunge-in defined as first periastron passage) particle 1 experiences a drag, whereas particle 2 experiences a thrust. This can be understood by the force due to the same posterior bulge of the envelope which pulls backward on particle 1 in its orbit.

To obtain an analytical expression for the drag force, we made use of the Bondi-Hoyle-Lyttleton formalism, and we considered different variations on that formalism (Edgar, 2004). Three quantities are needed for this: the particle velocity with respect to the ambient velocity of gas (formally the relative particle-gas velocity at infinity), the ambient gas density (formally the gas density at infinity), and the ambient sound speed (formally the gas sound speed at infinity). We also plot a modified version that accounts for the radial density gradient of the envelope (Dodd & McCrea, 1952).

2.4 Relative importance of z-components

Fig. 4: We compare the vertical components of the gas gravitational force on each particle and velocity of each particle with the component parallel to the orbital plane. We also compare the difference in vertical positions of the particles with the magnitude of their projected separation in the orbital plane. Finally we compare the components of the gravitational force of gas on each particle and particle velocity along the line separating the particles (subscript R) with its projection

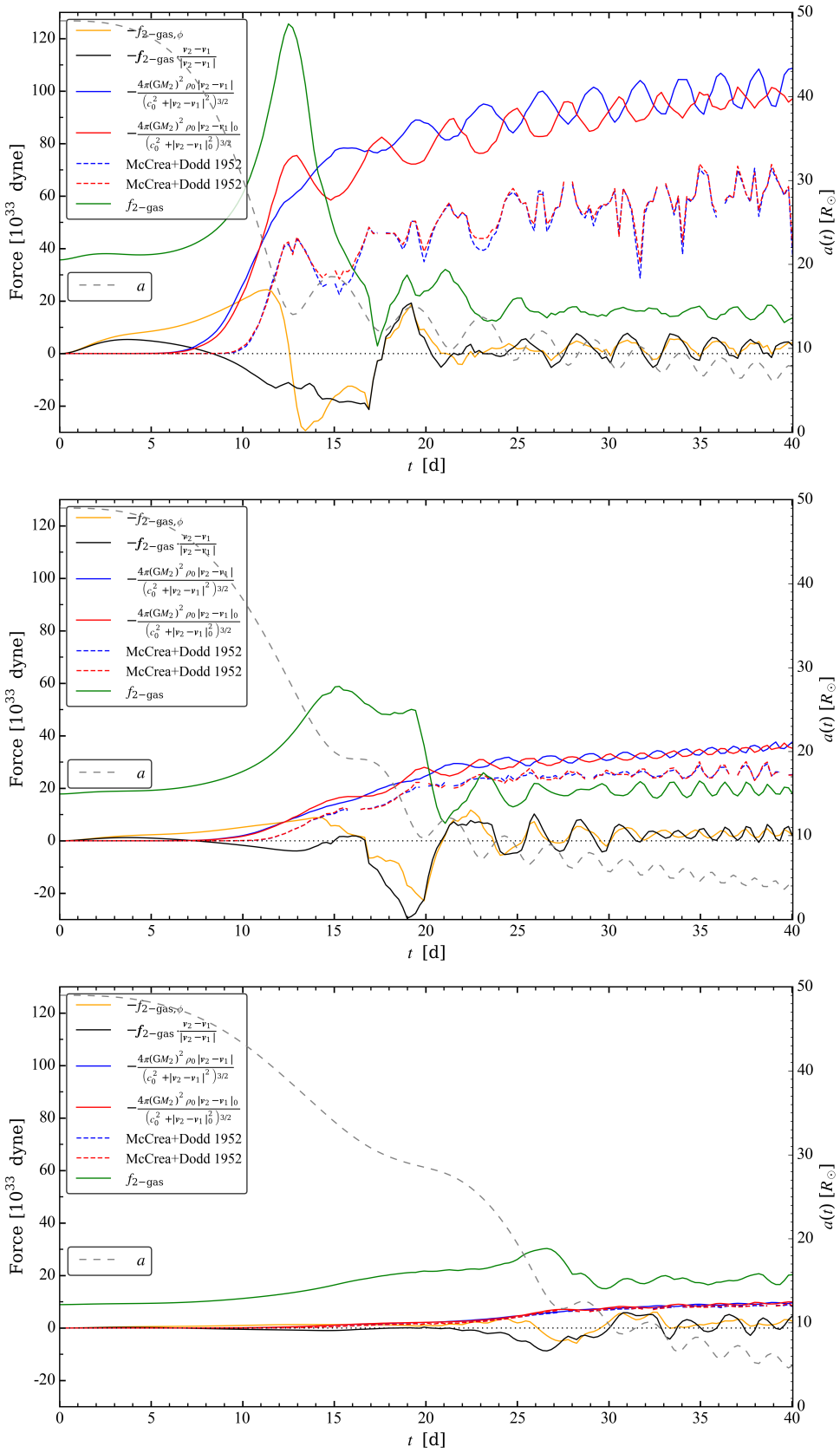

Figure 2: Force $\boldsymbol{f}_{2-\rm gas} \cdot (\boldsymbol{v_2} - \boldsymbol{v_1})/v$ and the component $f_{2-{\rm gas},\phi}$, where positive ϕ refers orbit about particle 1, in the same sense as the particles' orbit. Also shown are analytical expressions for the force amplitude (without the factor, > 1, equal to the logarithm of the ratio of outer and inner integration radii). A subscript "0" refers to the initial RGB profile at $t = 0$. For example $\rho_0(t) = \rho|_{t=0}[r = a(t)]$. These expressions are computed using the actual values of $\boldsymbol{v_2} - \boldsymbol{v_1}$ or the values $(\boldsymbol{v_2} - \boldsymbol{v_1})_0$, computed using the initial density profile of the RGB star, and assuming a circular orbit between the secondary and a point particle with mass equal to that of the primary core + the gas mass with $r < a(t)$. **Top:** Run 143, Fiducial run (Model A of Papers I and II), mass ratio $q = 0.5$. **Middle:** Run 149, $q = 0.25$. **Bottom:** Run 151, $q = 0.125$.

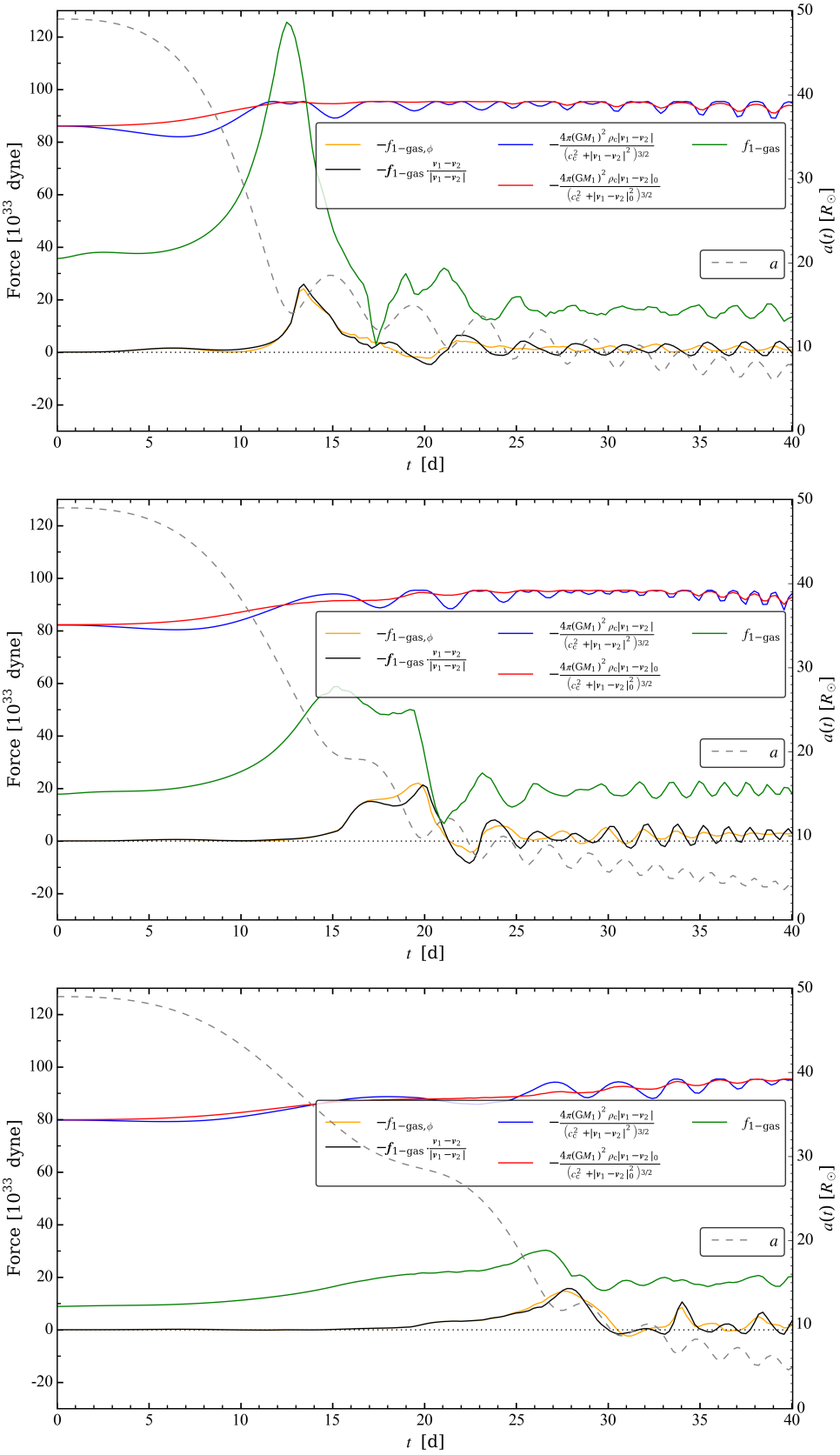

Figure 3: As Fig. 2 but now for particle 1. Here the subscript "c" refers to the value at the center of the initial RGB profile input into AstroBear. **Top:** Run 143, Fiducial run (Model A of Papers I and II), mass ratio $q = 0.5$. **Middle:** Run 149, $q = 0.25$. **Bottom:** Run 151, $q = 0.125$.

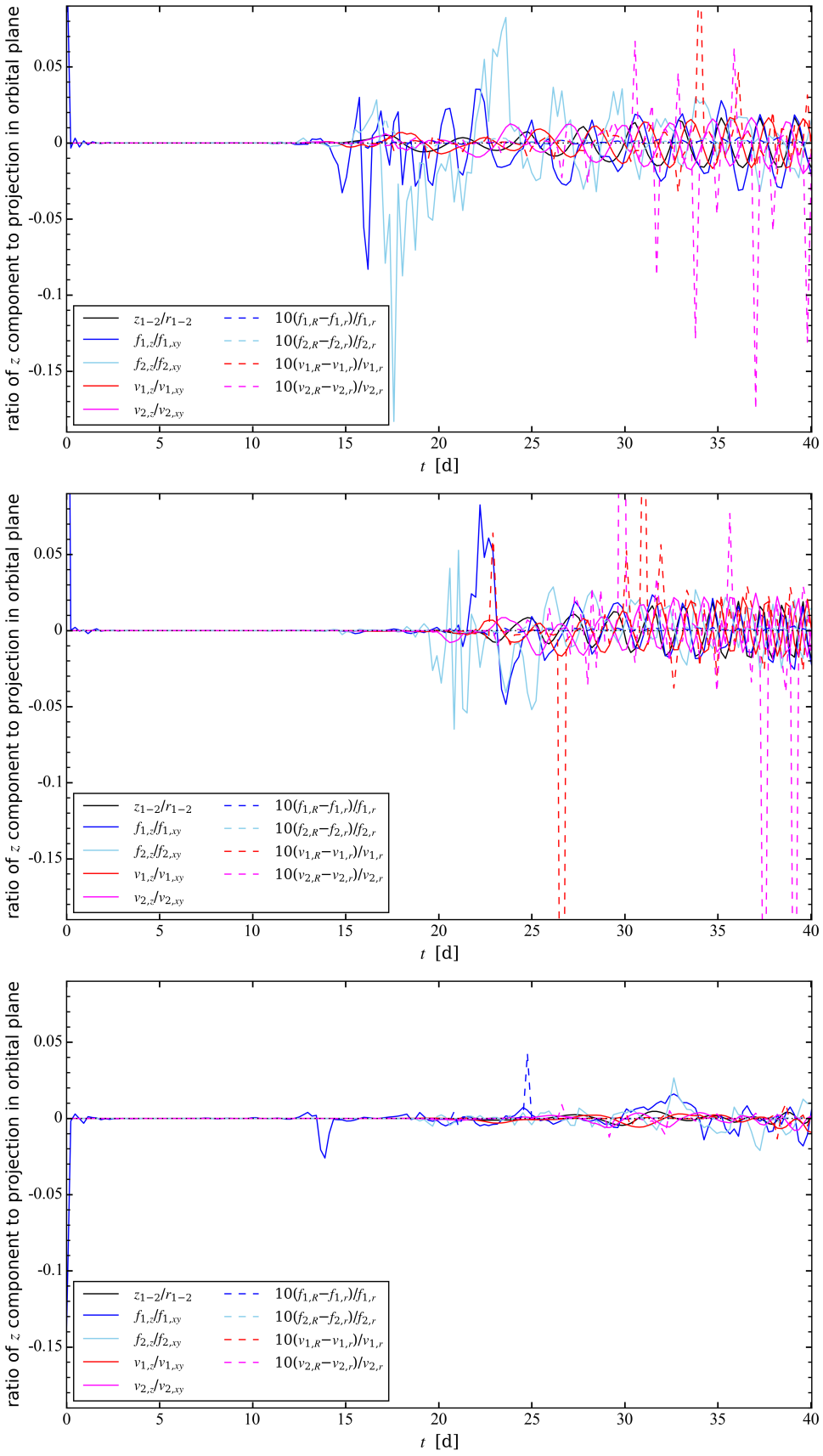

Figure 4: Ratios of various quantities plotted to gauge importance of vertical (z) component as compared to component in orbital (xy) plane. **Top:** Run 143, Fiducial run (Model A of Papers I and II), mass ratio $q = 0.5$. **Middle:** Run 149, $q = 0.25$. **Bottom:** Run 151, $q = 0.125$.

on the orbital plane (subscript r). Since these latter quantities turn out to be very small we multiply by 10 in the plot. We see that the vertical components are small, except, at times, the vertical gas force on particle 2, which has a maximum value of 19% of the component parallel to the orbital plane (light blue).

2.5 Velocities

Fig. 7: Velocities of the particles are calculated in two different ways. Either they are computed directly from the simulation data or they are calculated assuming a circular two-body orbit between the secondary and the mass of the primary that would be inside the actual orbit at time t had the envelope retained its original profile (velocities denoted by subscript '0').

$$v_{1,0} = \sqrt{\frac{Gm_2}{a}}\sqrt{\frac{m_2}{m_1+m_2}} = \sqrt{\frac{G\mu}{a}}\sqrt{\frac{m_2}{m_1}}, \tag{12}$$

where

$$\mu \equiv \frac{m_1 m_2}{m_1+m_2} \tag{13}$$

is the reduced mass. By symmetry,

$$v_{2,0} = \sqrt{\frac{Gm_1}{a}}\sqrt{\frac{m_1}{m_1+m_2}} = \sqrt{\frac{G\mu}{a}}\sqrt{\frac{m_1}{m_2}}, \tag{14}$$

and the velocites are in opposite directions. Note that here m_1 is the value of the interior envelope mass + core.

We see that the two different ways of calculating the velocities yield results that are in reasonable agreement.

To estimate the particle-gas velocity for gas at infinity, we have used the actual velocity of the particle either in the simulation (lab) frame or in the frame of the other particle (see Sec. 1) or we have used the velocity for a circular orbit at the actual separation assuming that the envelope still retained its initial profile.

To estimate the gas density at infinity, we have used the density at the actual separation in the initial envelope profile $\rho_0[a(t)]$.

To estimate the sound speed at infinity, we have used the sound speed at the actual separation in the initial envelope profile $c_0[a(t)]$, that is

$$c_0 = \left(\gamma\frac{P_0}{\rho_0}\right)^{1/2}, \tag{15}$$

where $\gamma = 5/3$ in our simulation, and P_0 and ρ_0 are taken from the original 1D MESA profile.

2.6 Bondi-Hoyle radius

Fig. 6 shows the BHL accretion radius. we see that $R_{\rm a}(t)$ is comparable to $a(t)$ (grey) and comparable to the pressure scale height of the initial profile $H_P[a(t)]$ (green), given by

$$H_0 = -P_0/(dP_0/dr)_0. \tag{16}$$

and also to the density scale height The density scale height

$$H_{\rho,0} = -\rho_0/(d\rho_0/dr)_0. \tag{17}$$

Thus, applying the Bondi-Hoyle-Lyttleton formalism to this case is rather questionable.

References

Dodd K. N., McCrea W. J., 1952, MNRAS, 112, 205

Edgar R., 2004, New Astron. Rev., 48, 843

MacLeod M., Antoni A., Murguia-Berthier A., Macias P., Ramirez-Ruiz E., 2017, ApJ, 838, 56

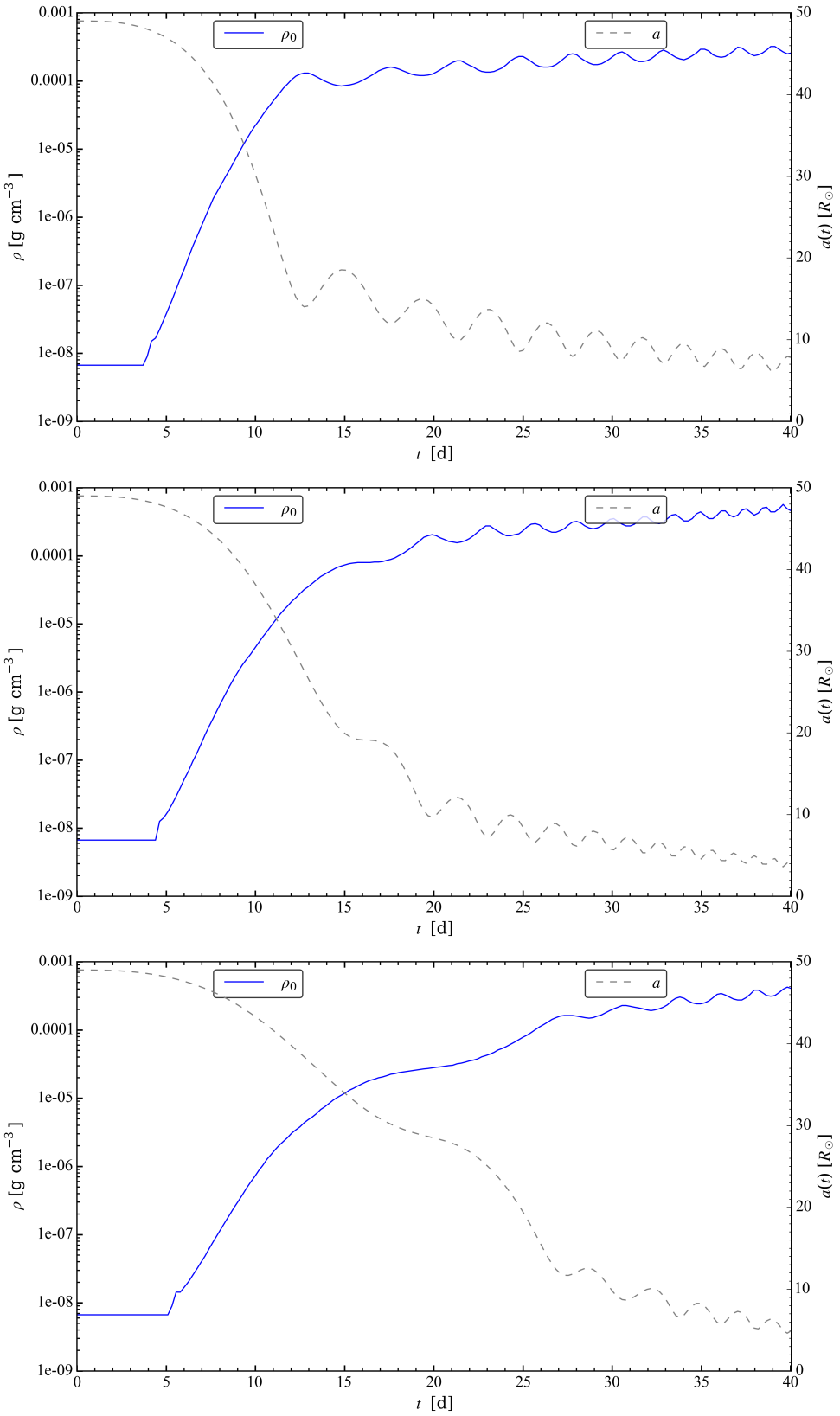

Figure 5: Density $\rho_0[a(t)]$. **Top:** Run 143, Fiducial run (Model A of Papers I and II), mass ratio $q = 0.5$. **Middle:** Run 149, $q = 0.25$. **Bottom:** Run 151, $q = 0.125$.

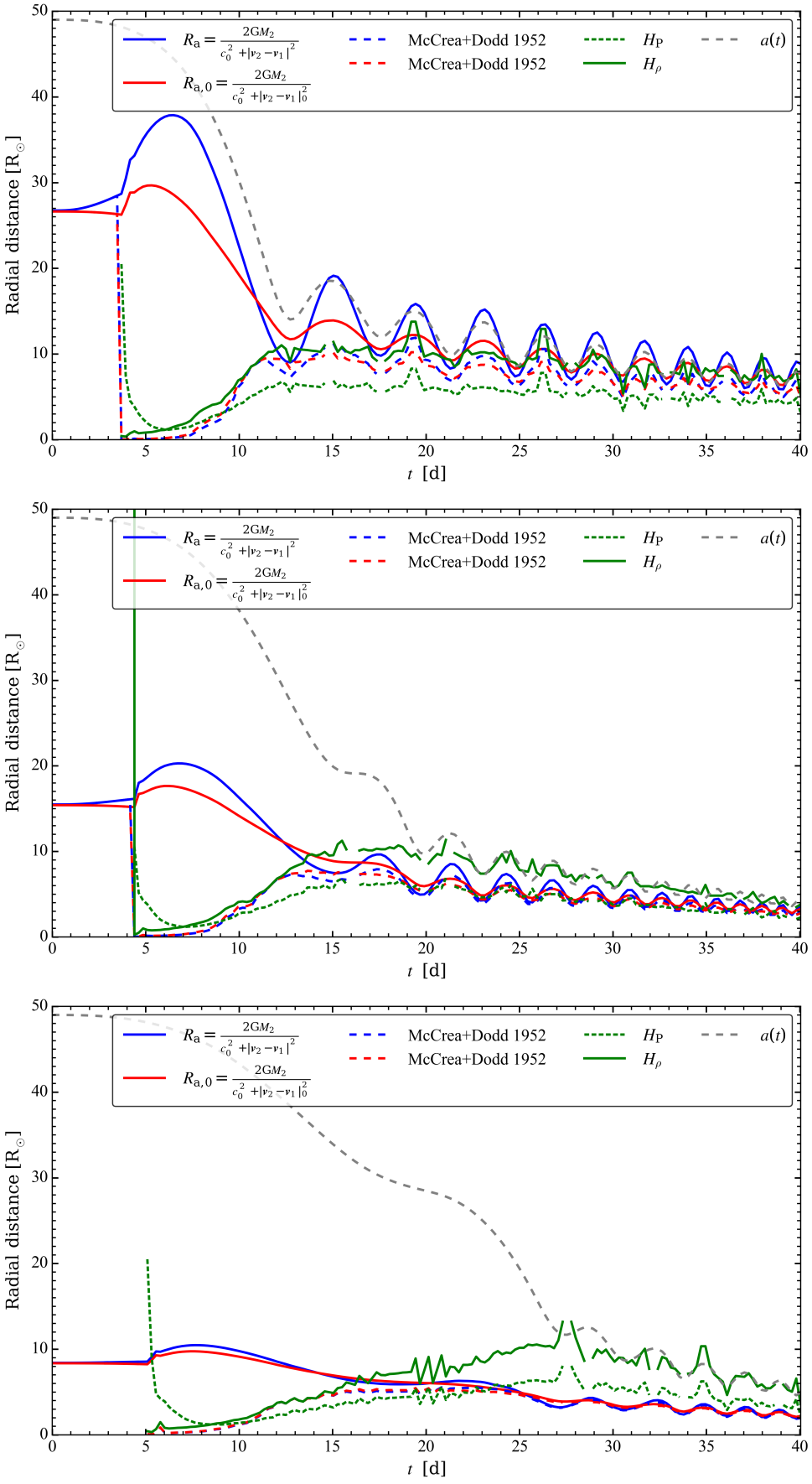

Figure 6: BHL accretion radius for particle 2, along with density and pressure scale heights. **Top:** Run 143, Fiducial run (Model A of Papers I and II), mass ratio $q = 0.5$. **Middle:** Run 149, $q = 0.25$. **Bottom:** Run 151, $q = 0.125$.

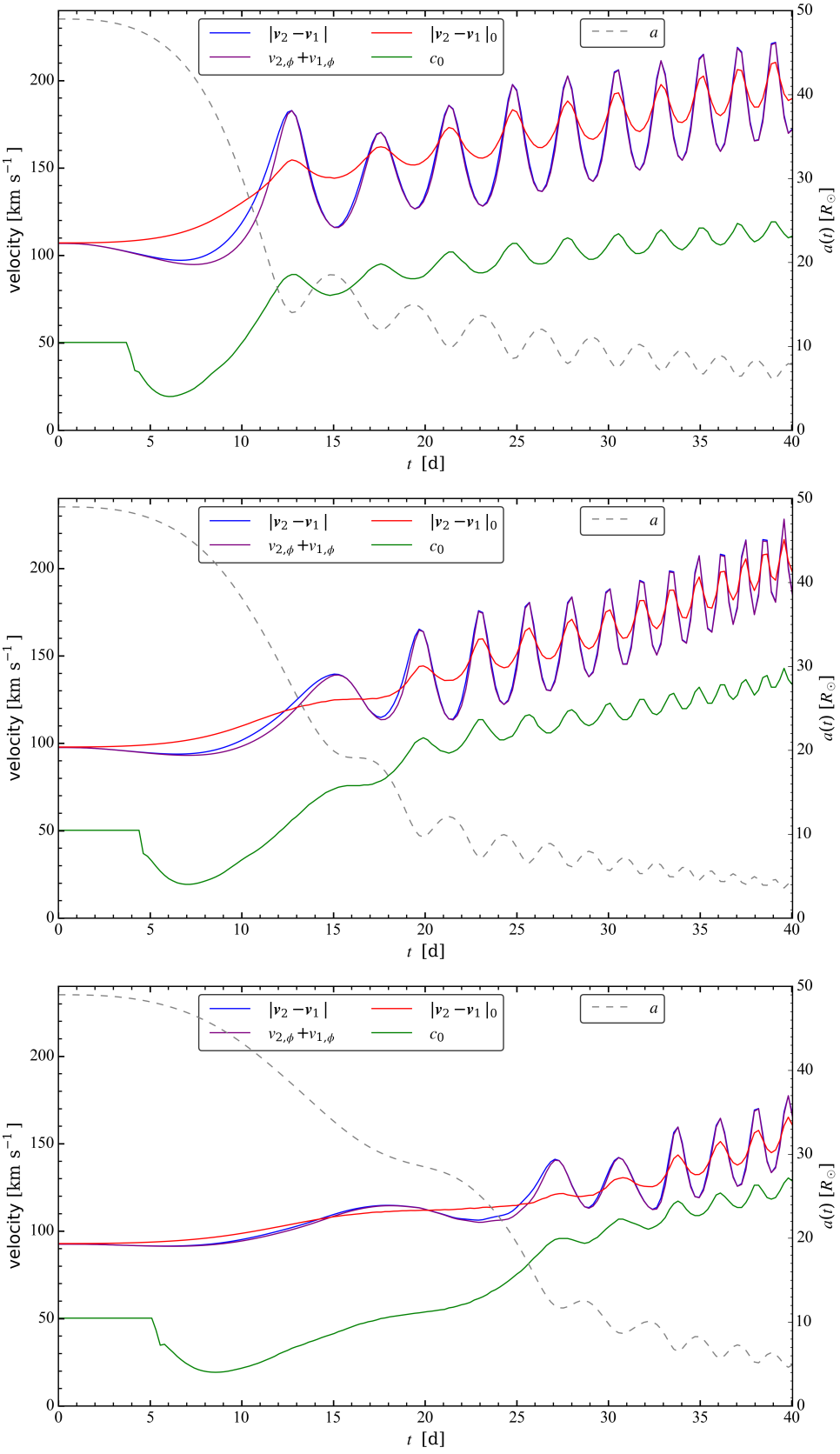

Figure 7: Particle velocities calculated from the simulation or estimated using initial profile. Those quantities estimated from the initial stellar profile are labeled with a '0' subscript. The sound speed is denoted by c. **Top:** Run 143, Fiducial run (Model A of Papers I and II), mass ratio $q = 0.5$. **Middle:** Run 149, $q = 0.25$. **Bottom:** Run 151, $q = 0.125$.

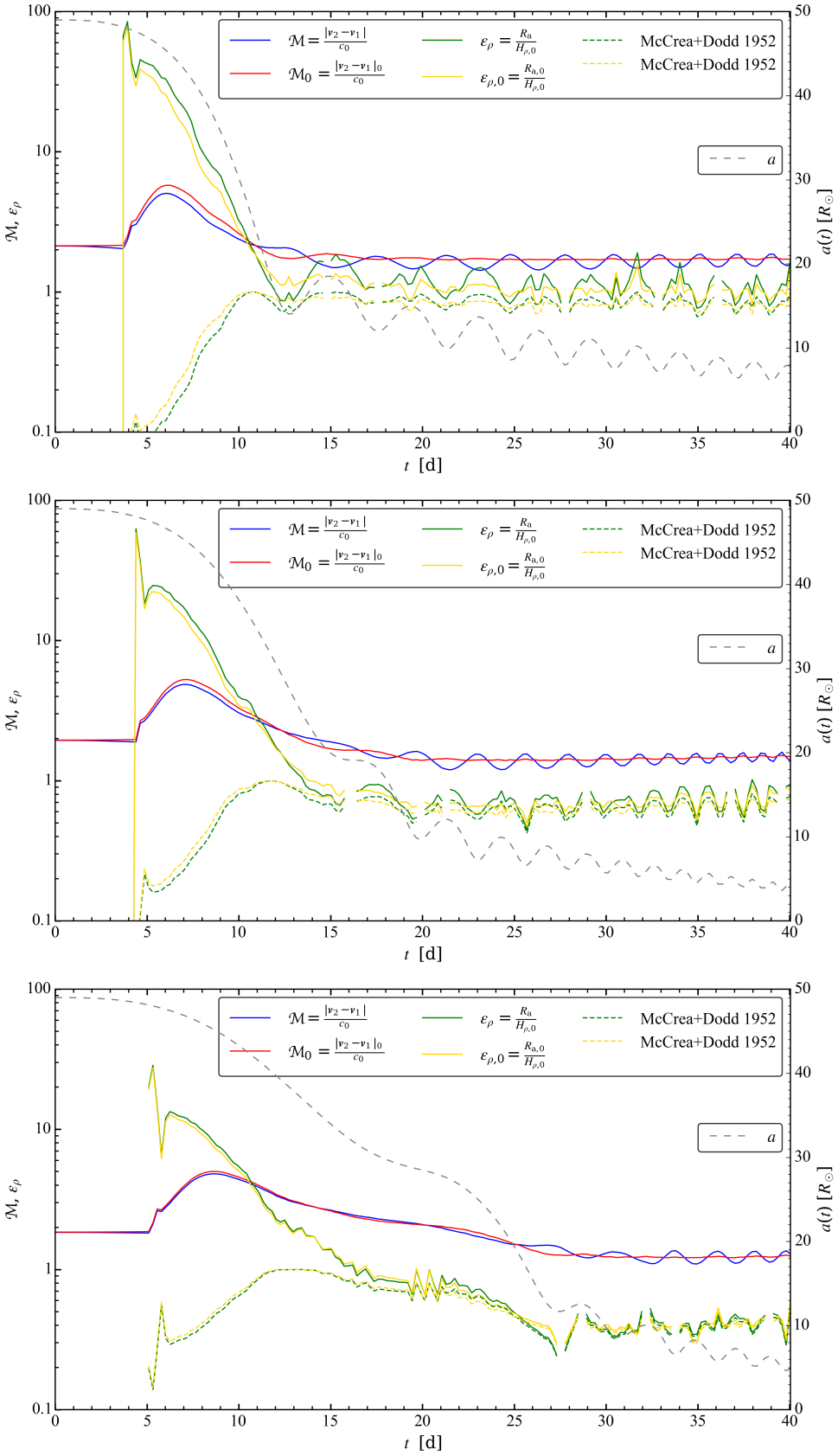

Figure 8: Mach number and ratio of BHL accretion radius to density scale height. **Top:** Run 143, Fiducial run (Model A of Papers I and II), mass ratio $q = 0.5$. **Middle:** Run 149, $q = 0.25$. **Bottom:** Run 151, $q = 0.125$.